Peak deviator stress and strain uncertainty of isotropically consolidated triaxial compression tests on saturated non-cohesive soils

Aikaterini (Renata) Miliopoulou

Fugro GB Limited, Fugro House, Hithercroft Road, Wallingford OX10 9RB, UK
a.miliopoulou@fugro.com

ABSTRACT

This paper presents the methodology for calculating the peak deviator stress and strain at peak deviator stress uncertainty of triaxial compression tests on water saturated, non-cohesive soils consolidated under isotropic conditions. A silicious sand sample is prepared in the same way to produce identical cylindrical specimens. These are then tested under the same conditions. Type A and type B uncertainty are calculated separately and used to yield the combined and expanded uncertainty of the main results, peak deviator stress and strain at peak deviator stress. For both measurands, type A uncertainty is significantly higher that type B and it is the factor mainly affecting the overall uncertainty of the results.

Keywords: uncertainty; triaxial tests; deviator stress; strain.

1. Introduction

When all of the known or suspected components of error have been evaluated and the appropriate corrections have been applied, there still remains an uncertainty about the correctness of the stated result, that is, a doubt about how well the result of the measurement represents the value of the quantity being measured. (IPM et al. 2008, 0.2). In order for a measurement result to be meaningful, it must be accompanied by a quantified indication of its quality and reliability. This is the measurement uncertainty.

While the concept of error has always been considered when making measurements and reporting results, uncertainty is a more recent approach. Error focuses on the worst case and aims to determine the maximum possible error so that any conclusions tend towards the conservative. Uncertainty focuses on probability. The aim is to determine the most probable range for the result and the possibility of a measurement lying outside this range. (IPM et al. 2008).

The term "uncertainty" might be perceived as a theoretical and qualitative one. Yet IPM et al. (2008) gather all the principles and present in detail the methodology to be followed to determine measurement uncertainty. The metrologist needs a thorough understanding of the measurement to initially identify and then quantify the parameters that influence its uncertainty. IPM et al. (2008) refer to the "art of measurement" because both an insight into the depths of the measuring model and a good understanding of the mathematical tools necessary to describe the measurement and its uncertainty are required.

Accredited laboratories are required to determine measurement uncertainty. However, as geotechnical test results do not have to comply with specification limits or legal requirements, uncertainty is rarely reported.

The triaxial compression test is fundamental in geotechnical engineering. The information this provides on the mechanical properties of soils helps foundation designers to understand how the soils investigated would behave under stress. This paper presents the methodology used to determine the uncertainty of the two basic results of a triaxial test, peak deviator stress and strain at peak deviator stress. The principles of triaxial tests are described first, together with the conditions applied. Then the focus moves to the mathematical models for determining the uncertainty of the results, the assumptions for calculating uncertainty, and the final uncertainty values. Finally, the outcome and potential future steps are discussed.

2. Triaxial tests

A measurement begins by specifying the measurand, the method of measurement, and the measurement procedure. (IPM et al. 2008, 3.1.1).

2.1. Basic principles of triaxial tests

The objective of triaxial testing is to assess the mechanical properties of a cylindrical soil specimen. Testing is performed within a cell where the pressure can be controlled and maintained. The pressure is often set to replicate the in-situ conditions of the soil. The specimen, confined within a watertight membrane, is initially saturated so that all air voids are filled with water, then consolidated to return to its in-situ stress conditions. Finally, during the compression stage, force is applied vertically to the sample in either drained or undrained conditions. During the compression stage, several parameters are measured and the test continues until the sample fails. The peak deviator stress and the strain at peak deviator stress are calculated as the main results.

Triaxial compression tests are carried out as described in ISO 17892-9:2018 (ISO 2018).

2.2. Measurement equipment and resolution

The initial sample dimensions are measured with electronic calipers, reading to 0.01 mm and accurate to 0.05 mm.

The applied vertical force is measured through load cells, which are compensated for the applied pressures. The load cells are of various capacities; the maximum accepted error is 1% of the applied load for force measurements above 10% of their capacity.

Linear displacement transducers reading to 0.001 mm and accurate to 0.1 mm are used to measure the change in height of the specimen.

Automatic volume change apparatus or pressure controllers, both reading to 0.001 cm^3 and accurate to 0.2 cm^3, measure the change in volume caused by water moving in or out of the sample.

Pressure transducers of various capacities measure pore-water pressure and cell pressure. The transducers have a resolution from 1 kPa to 2 kPa depending on their capacity. The maximum accepted error is 0.25% of the transducer's full range, which might be up to 7.5 kPa for a 3000 kPa transducer.

3. Exercise layout

The total number of tests included in this paper is 140. Tests were conducted from June 2020 until September 2023 by 17 technicians, using 34 different triaxial testing systems with a variety of measuring devices.

3.1. Material used

A washed, dried, and closely graded silica sand with a 99.8% content of SiO_2 was used to prepare the specimens. The sand originated from the Lower Greensand Formation in Bedfordshire, UK. Its particles were rounded to subangular, with a grading of more than 99% passing 600 μm and less than 1% passing 63 μm. The particle density was 2.65 gr/cm^3.

3.2. Test conditions

The sand samples were wetted to an initial moisture content of 10% by mass and compacted to an initial dry density of 1.60 ± 0.2 gr/cm^3 using the Ladd undercompaction method (Ladd 1978). The cell pressure was set to 150 kPa. Initial saturation was performed either by incremental increase or by slowly ramped increase of pressure. Consolidation was then carried out under isotropic conditions, with the pressure applied to the sample being the same in all three directions. Shearing was performed under drained conditions, allowing water to flow freely out of the sample and maintaining constant pore water pressure during compression.

The laboratory's temperature was maintained between 18°C and 22°C throughout the tests.

3.3. Formulas for peak deviator stress and strain

Deviator stress is calculated from the force applied to the specimen divided by the area to which that force is applied – the cross-sectional area of the cylindrical specimen. During a drained test, this area changes as the sample is compressed, based on the change in height of the sample and the volume change caused by water moving out of the sample. Strain, as a percentage, is calculated by dividing the change of height of the specimen by its initial height. The relevant formulas are all given in the testing standard. The peak deviator stress and strain at peak deviator stress are calculated from quantities directly measured during the test. The main measurement models are presented in Section 5.1.

4. Principles and methodology for measurement uncertainty

Although taking measurements is a specified, strict process, the results are heavily driven by statistics. This is because the metrologist needs to evaluate whether the data obtained during experiments reflect reality or if they are random deviations from it. This is the reason why the result of a measurement is not univocal. It depends on several parameters and thus can be considered a stochastic variable (Mathioulakis 2004).

4.1. Basic concepts of uncertainty

The basic mathematical model for a measurand is shown in Eq. (1), where Y is the measurand and X_i are N quantities Y is determined from. Considering xi as the best estimate for X_i, then the best estimate of Y is y.

$$Y = f(X_1, X_2, \dots, X_N) \rightarrow y = f(x_1, x_2, \dots, x_N) \quad (1)$$

Uncertainty is divided in two types, type A and type B, indicating the two different ways of evaluating uncertainty components. A type A standard uncertainty is obtained from a probability density function derived from an observed frequency distribution, while a type B standard uncertainty is obtained from an assumed probability density function based on the degree of belief that an event will occur. Both types of evaluation are based on probability distributions, and the uncertainty components resulting from either type are quantified by variances or standard deviations (IPM et al. 2008). Strictly by definition, uncertainty is the standard deviation of the distributions mentioned above. Variance, the standard deviation squared, is a more fundamental property and more widely used as a measure of the uncertainty. In the following sections, the term 'uncertainty' is used to mean both the variance and the standard deviation. Symbols, squared or not, indicate exactly which. All steps up to combined uncertainty are referred to in terms of variance, and the final expanded uncertainty is referred to in terms of standard deviation.

To be more precise, the distinction between type A and B uncertainties should not focus on their nature, as they are both probability density functions. It should focus on the way they are estimated (Mathioulakis 2004).

The combined standard uncertainty arises from multiple input quantities and is determined by considering all variance and covariance components through the application of the law of propagation of uncertainty.

The expanded uncertainty is finally calculated, choosing a coverage factor, to provide a range of values most likely to include the measurement result.

4.2. Type A uncertainty

Considering normal distribution, in a set of n repeated, independent observations of quantity q under the same conditions, the best estimate of q is their average according to Eq. (2).

$$\bar{q} = \sum_{k=1}^{n} q_k \quad (2)$$

The type A uncertainty of q is given by the variance of the mean $s^2(\bar{q})$ as shown in Eq. (3).

$$s^2(\bar{q}) = \frac{s^2(q_k)}{n} = \frac{1}{n(n-1)} \sum_{j=1}^{n} (q_j - \bar{q})^2 \quad (3)$$

To evaluate type A uncertainty, independent observations must be performed under repeatability conditions to ensure that the results are not influenced by systematic components. Moreover, this type of uncertainty does not give any information on the reliability of the method or the measuring apparatus and can produce distorted results when the observations are less than 10 (Mathioulakis 2004).

4.3. Type B uncertainty

When repeated observations are not feasible, the metrologist needs to find other sources to evaluate uncertainty. These might include previous experience, manufacturer specifications, calibration certificates, limitation of use based on operation principles, and more. The only example described here, which is commonly used, is the declared error. Where it is stated that the value of X_i lies within the interval of ± b, there is 100% probability that X_i is between $x_i - b$ and $x_i + b$. Without knowing where exactly in this range the value of X_i might be, x_i follows a rectangular distribution and the associated variance is given in Eq. (4).

$$u^2(x_i) = \frac{(2b)^2}{12} \rightarrow u^2(x_i) = \frac{b^2}{3} \quad (4)$$

4.4. Combined uncertainty

Following the Eq. (1) model, the combined standard uncertainty of y, $u_c(y)$, is obtained using the law of propagation of uncertainty. According to it, the combined standard uncertainty is the positive square root of the combined variance $u_c^2(y)$, given in Eq. (5) where $u(x_i, x_j)$ is the estimated covariance associated with x_i and x_j, and is given as a function of the correlation coefficient r in Eq. (6).

$$u_c^2(y) = \sum_{i=1}^{N} \left(\frac{\partial f}{\partial x_i}\right)^2 u^2(x_i) + \sum_{i=1}^{N-1} \sum_{j=i+1}^{N} \frac{\partial f}{\partial x_i} \frac{\partial f}{\partial x_j} u(x_i, x_j) \quad (5)$$

$$r(x_i, x_j) = \frac{u(x_i, x_j)}{u(x_i) u(x_j)} \quad (6)$$

Where all x_i variables are independent, then $r(x_i, x_j) = 0$ and Eq. (5) is simplified to Eq. (7).

$$u_c^2(y) = \sum_{i=1}^{N} \left(\frac{\partial f}{\partial x_i}\right)^2 u^2(x_i) \quad (7)$$

To calculate the combined uncertainty, all incoming uncertainties must have the same probability and refer to the same confidence interval. Whether they are type A or type B is irrelevant.

4.5. Expanded uncertainty

The expanded uncertainty U is obtained by multiplying the combined standard uncertainty $u_c(y)$ by a coverage factor k according to Eq (8).

$$U(y) = k u_c(y) \quad (8)$$

The result of a measurement is then conveniently expressed as Y = $y \pm U$, which is interpreted to mean that the best estimate of the value attributable to the measurand Y is y, and that $y - U$ to $y + U$ is an interval that may be expected to encompass a large fraction of the distribution of values that could reasonably be attributed to Y (IPM et al. 2008, 6.2.1).

5. Deviator stress and strain results

5.1. Measurement model

The measurement models for peak deviator stress and strain at peak deviator stress, following the ISO 17892-9:2018 (ISO 2018) standard test method, are given in Eq. (9) and (10).

$$\sigma_v = \frac{4000F(H_0 - \Delta H)}{\pi D_0^2 H_0 - 4\Delta V} \rightarrow \sigma_v = f(F, H_0, \Delta H, D_0, \Delta V) \quad (9)$$

$$\varepsilon = \frac{\Delta H}{H_0} 100 \rightarrow \varepsilon = f(H_o, \Delta H) \quad (10)$$

Where:

- σ_v (kPa) is the peak deviator stress;
- F (N) is the force applied at peak stress;
- H_0 (mm) is the initial height of the specimen;
- ΔH (mm) is the change in height of the specimen at peak deviator stress;
- D_0 (mm) is the initial diameter of the specimen;
- ΔV (mm^3) is the change in volume of the specimen caused by the drainage of water;
- ε (%) is the strain, the percentage of change in height of the specimen at peak deviator stress.

5.2. Test results

Fig. 1 and 2 present peak deviator stress and strain results.

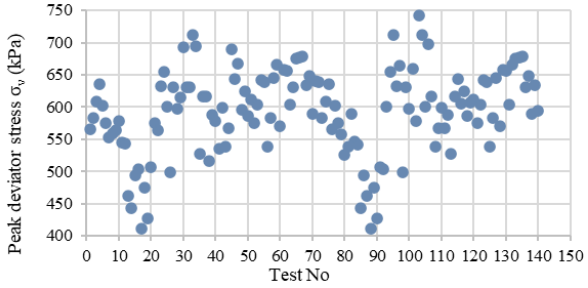

Figure 1. Peak deviator stress σ_v (kPa) results

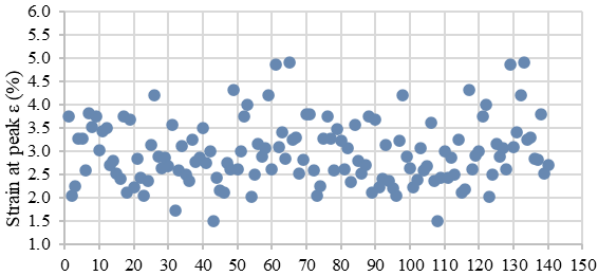

Figure 2. Strain at peak deviator stress ε (%) results

Probability density distribution charts were used to check the results for symmetry and quantile–quantile plots to check for normality. All the results were found to follow normal distribution as shown in Fig. 3 and 4.

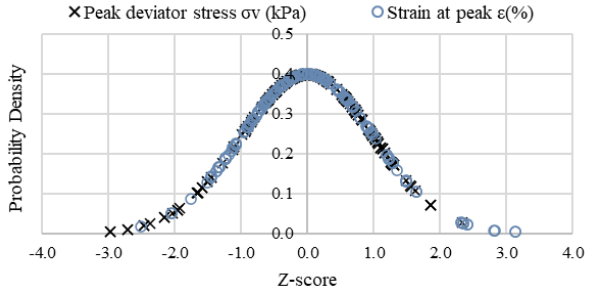

Figure 3. Distribution of test results

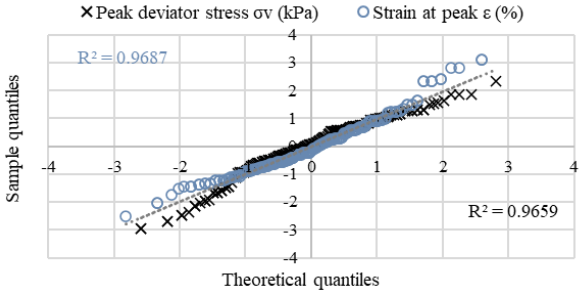

Figure 4. Quantile-Quantile (QQ) plot of test results.

6. Type A uncertainty

6.1. Calculation of type A uncertainty

When the objective is to calculate the uncertainty of a method, type A uncertainty should be evaluated under repeatability conditions where the operator carries out repeated tests on the sample within a short period of time, under the same conditions and using the same equipment, as outlined in ISO 5725-1:2023 (ISO 2023). However, the objective in this exercise is to evaluate the uncertainty of the laboratory, accounting for all involved equipment and personnel, under intermediate precision conditions.

Several different intermediate checks were made with the available data. Type A uncertainty for peak deviator stress and strain at peak deviator stress was calculated for individual technicians using a number of testing systems and for a number of technicians using individual testing systems. The results are presented in tables 1 and 2 respectively.

Table 1. Type A uncertainty for technicians

Technician	No of systems	No of tests	σ_v (kPa) average	$s^2(\sigma v)$	ε (%) average	$s^2(\varepsilon)$
T1	7	18	593.8	103.7	2.7590	0.0237
T2	10	21	555.3	122.2	3.0745	0.0105
T3	12	29	572.9	289.1	3.2499	0.0165
T4	6	16	604.0	162.4	2.8598	0.0092

Table 2. Type A uncertainty for systems

System	No of technicians	No of tests	σ_v (kPa) average	$s^2(\sigma v)$	ε (%) average	$s^2(\varepsilon)$
S1	4	17	538.3	424.1	3.2773	0.0303
S2	4	13	605.3	219.0	2.8998	0.0673

The above tables indicate that equipment variance is a little higher than the personnel variance.

Type A uncertainty was eventually calculated from the whole data set of 140 test results.

6.2. Type A uncertainty results

Based on the above methodology and assumptions, type A uncertainty is $u_A^2(\sigma_v) = 31.269\,kPa^2$ for peak deviator stress and $u_A^2(\varepsilon) = 0.003344\,\%^2$ for strain at peak deviator stress.

These results are considerably lower than the results shown in Tables 1 and 2. They incorporate significantly more variables, technicians and testing systems, but they are in total a lot more. The increased number of test results in principle lowers the uncertainty and gives an overall better estimation of how the measurands behave.

7. Type B uncertainty

7.1. Calculation of type B uncertainty from the mathematical model

Following the mathematical models set in Eq. (9) and (10), it is evident that each of the measuring devices contributes its own uncertainty to the overall uncertainty of the output value of peak deviator stress and strain at peak deviator stress. The law of propagation of uncertainty, as shown in Eq. (5) using also Eq. (6), is in this case applied to calculate the type B uncertainty of peak deviator stress and strain at peak deviator stress as shown in Eq. (11) and (12) respectively.

$$
\begin{aligned}
u_B^2(\sigma_v) = {} & \left(\frac{\partial \sigma_v}{\partial F}\right)^2 u^2(F) + \left(\frac{\partial \sigma_v}{\partial H_0}\right)^2 u^2(H_0) + \\
& \left(\frac{\partial \sigma_v}{\partial \Delta H}\right)^2 u^2(\Delta H) + \left(\frac{\partial \sigma_v}{\partial D_0}\right)^2 u^2(D_0) + \left(\frac{\partial \sigma_v}{\partial \Delta V}\right)^2 u^2(\Delta V) + \\
& 2\left(\frac{\partial \sigma_v}{\partial F}\right)\left(\frac{\partial \sigma_v}{\partial H_0}\right) r(F, H_0) u(F) u(H_0) + \\
& 2\left(\frac{\partial \sigma_v}{\partial F}\right)\left(\frac{\partial \sigma_v}{\partial \Delta H}\right) r(F, \Delta H) u(F) u(\Delta H) + \\
& 2\left(\frac{\partial \sigma_v}{\partial F}\right)\left(\frac{\partial \sigma_v}{\partial D_0}\right) r(F, D_0) u(F) u(D_0) + \\
& 2\left(\frac{\partial \sigma_v}{\partial F}\right)\left(\frac{\partial \sigma_v}{\partial \Delta V}\right) r(F, \Delta V) u(F) u(\Delta V) + \\
& 2\left(\frac{\partial \sigma_v}{\partial H_0}\right)\left(\frac{\partial \sigma_v}{\partial \Delta H}\right) r(H_0, \Delta H) u(H_0) u(\Delta H) + \\
& 2\left(\frac{\partial \sigma_v}{\partial H_0}\right)\left(\frac{\partial \sigma_v}{\partial D_0}\right) r(H_0, D_0) u(H_0) u(D_0) + \\
& 2\left(\frac{\partial \sigma_v}{\partial H_0}\right)\left(\frac{\partial \sigma_v}{\partial \Delta V}\right) r(H_0, \Delta V) u(H_0) u(\Delta V) + \\
& 2\left(\frac{\partial \sigma_v}{\partial \Delta H}\right)\left(\frac{\partial \sigma_v}{\partial D_0}\right) r(\Delta H, D_0) u(\Delta H) u(D_0) + \\
& 2\left(\frac{\partial \sigma_v}{\partial \Delta H}\right)\left(\frac{\partial \sigma_v}{\partial \Delta V}\right) r(\Delta H, \Delta V) u(\Delta H) u(\Delta V) + \\
& 2\left(\frac{\partial \sigma_v}{\partial D_0}\right)\left(\frac{\partial \sigma_v}{\partial \Delta V}\right) r(D_0, \Delta V) u(D_0) u(\Delta V)
\end{aligned}
\tag{11}
$$

$$
\begin{aligned}
u_B^2(\varepsilon) = {} & \left(\frac{\partial \varepsilon}{\partial H_0}\right)^2 u^2(H_0) + \left(\frac{\partial \varepsilon}{\partial \Delta H}\right)^2 u^2(\Delta H) + \\
& 2\left(\frac{\partial \varepsilon}{\partial H_0}\right)\left(\frac{\partial \varepsilon}{\partial \Delta H}\right) r(H_0, \Delta H) u(H_0) u(\Delta H)
\end{aligned}
\tag{12}
$$

Where:

- $u(F)$ is the uncertainty of load, equal to the uncertainty of the load cell;
- $u(H_0)$ is the uncertainty of the initial height, equal to the uncertainty of the caliper;
- $u(\Delta H)$ is the uncertainty of the change in height, equal to the uncertainty of the linear displacement transducer;
- $u(D_0)$ is the uncertainty of the initial diameter, equal to the uncertainty of the caliper;
- $u(\Delta V)$ is the uncertainty of the change in volume, equal to the uncertainty of the volume transducer.

Except for the mathematical transformations to calculate the partial derivatives in Eq. (11) and (12), the

other parameters needed to acquire type B uncertainty are the uncertainty of each measuring device, derived from its calibration records and the correlation coefficients r between the individual variables. These are described in the following paragraphs.

7.2. Calculation of equipment uncertainty

Any error found in measuring equipment should be corrected before uncertainty is calculated (IPM et al. 2008). However, it is not possible to correct the errors of the measuring equipment used in triaxial tests. All the measuring devices described in Section 2.3 operate within a range and are calibrated at specified intervals. From these points a linear correlation a factor is derived and applied for the whole range. But this carries on an error, as the relationship is never perfectly linear.

Since errors cannot be corrected, they must be accounted for within the uncertainty of the measuring device. This has the unfortunate outcome that uncertainty is both overestimated and averaged over a range of results, thus increasing its value.

The methodology described in IPM et al. (2008, F.2.4.5) was followed for including the error in the uncertainty budget. The other parameters included in it are the error and uncertainty of the reference equipment used, the standard deviation of the mean for repeated measurements, and the device resolution. The uncertainty results for force, change in height and volume, in terms of variance, are presented in Fig. 5, 6 and 7.

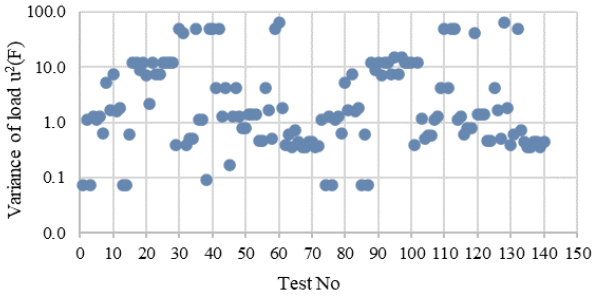

Figure 5. Variance of load

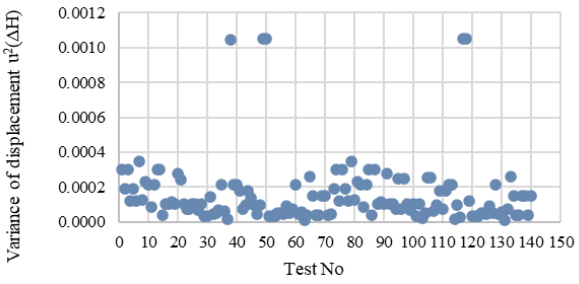

Figure 6. Variance of change in height

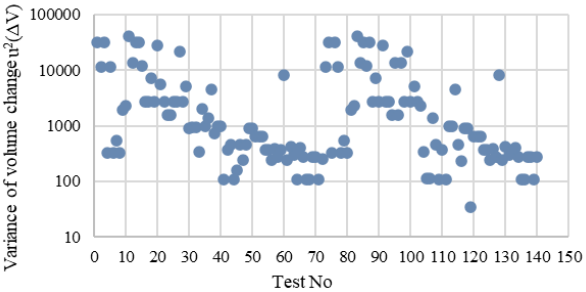

Figure 7. Variance of volume

As there are few calipers in the laboratory and it was not possible to trace which were used for each test, all the uncertainties for the calipers were calculated from calibrations done over the duration during which the tests were performed, by the same methodology. Their average was used as the uncertainty of the initial height $u(H_0)$ and diameter $u(D_0)$ of the sample. That value, in terms of variance, is shown in Eq. (13).

$$u^2(H_0) = u^2(D_0) = u^2(Calipers) = 0.000041\ mm^2 \quad (13)$$

One assumption made in this methodology is that the error is a linear function of the reference equipment units, introducing one more uncertainty parameter as this is not always the case. This uncertainty parameter was not quantified in this experiment as it was deemed insignificant compared with the others.

7.3. Calculation of correlation coefficients

The variables for calculating deviator stress and strain during triaxial tests cannot be considered independent. For deviator stress, the initial diameter and height are dependent on each other, as samples have a defined diameter to height ratio in the testing standard. Load, changes in height and volume changes are measured simultaneously during the same shearing process on the same sample. Similarly, for strain, change in height is dependent on the initial height.

This qualitative suspicion was verified by following the Pearson correlation method. Although this method assumes linearity, it gives a strong indication of correlation and is suggested by IPM et al. (2008). According to it, two variables, x_1 and x_2, measured in k pairs with respectively $\overline{x_1}$ and $\overline{x_2}$ averages, have a correlation coefficient as shown in Eq. (14).

$$r(x_1, x_2) = \frac{\sum(x_1 - \overline{x_1})\,(x_2 - \overline{x_2})}{\sqrt{\sum(x_1 - \overline{x_1})^2 \sum(x_2 - \overline{x_2})^2}} \quad (14)$$

The correlation coefficients were calculated by applying Eq. (14) to the data from the 140 tests and are presented in Table 3.

Table 3. Correlation coefficients

Correlation coefficient	Value	Correlation coefficient	Value
$r(F, H_0)$	0.805378	$r(H_0, D_0)$	0.915558
$r(F, \Delta H)$	0.319700	$r(H_0, \Delta V)$	0.496690
$r(F, D_0)$	0.797554	$r(\Delta H, D_0)$	0.280781
$r(F, \Delta V)$	0.519739	$r(\Delta H, \Delta V)$	0.551701
$r(H_0, \Delta H)$	0.322815	$r(D_0, \Delta V)$	0.452457

Normally a correlation coefficient below 0.3 implies a weak relationship between the two variables, between 0.3 and 0.5 a moderate relationship, and above 0.5 a strong one.

7.4. Type B uncertainty results

All the data necessary to calculate type B uncertainty for every separate test, following Eq. (11) for peak deviator stress and Eq. (12) for strain at peak deviator stress, were obtained by following the process outlined above.

7.4.1. Type B uncertainty for peak deviator stress

Equation (11) is the sum of 15 different summands, each derived from a different source of uncertainty.

These summands are calculated and presented separately to make it possible to identify which factors have a greater effect on the final uncertainty. The first five summands are labelled as v and the correlated summands as r. They appear in Eq. (11) in the order they are presented in Fig. 8 and 9. The first factor for load has been separated as those results were significantly different.

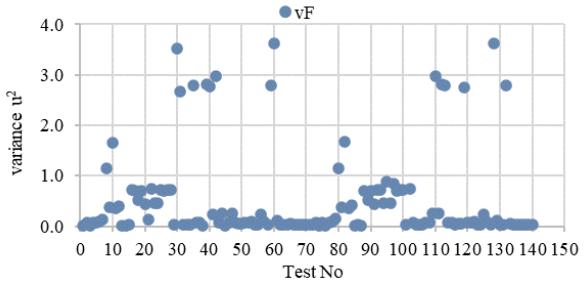

Figure 8. Variance due to force

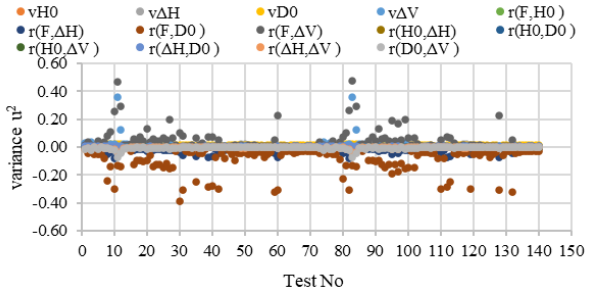

Figure 9. Variance due to all factors in Eq. (11)

While not all the factors are clearly distinguished, it is evident that most fluctuate very close to 0, with some varying between − 0.2 and + 0.2. The force uncertainty is an order of magnitude higher, with most values between 0 and 2 and some as high as 4.

The total type B uncertainty based on the individual equipment used, calculated by applying Eq. (11) and summing all parts, is presented in Fig. 10.

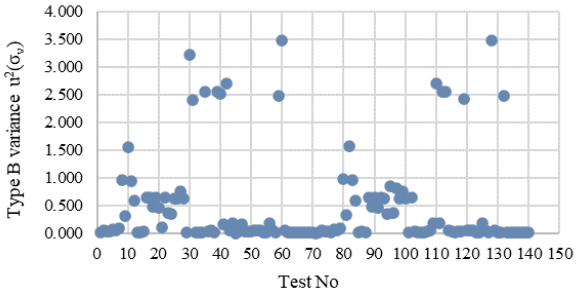

Figure 10. Type B uncertainty for peak deviator stress

A comparison of graphs 8, 9 and 10 shows that force is the most significant factor affecting type B uncertainty. All other factors have less influence.

7.4.2. Type B uncertainty for strain at peak deviator stress

The three summands of Eq. (12) are plotted separately in order to identify the parameter that has the most significant effect on type B uncertainty for strain. These summands are shown in Fig. 11.

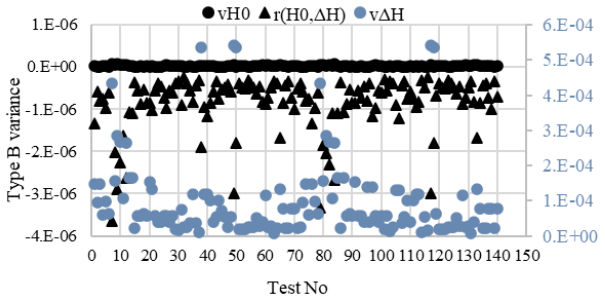

Figure 11. Variance due to all factors in Eq. (12) for strain

Fig. 11 shows that, for strain at peak deviator stress, each parameter is affected to a different order of magnitude: uncertainty due to initial height is calculated to the 8th decimal; uncertainty due to covariance of initial height and change in height is calculated to the 6th decimal; and uncertainty due to change in height is calculated to the 4th decimal. Thus the last one is significantly impacting type B uncertainty for strain.

The overall type B uncertainty for strain is plotted in Fig. 12 and, as expected, overall type B for strain is almost equal to uncertainty due to change in height.

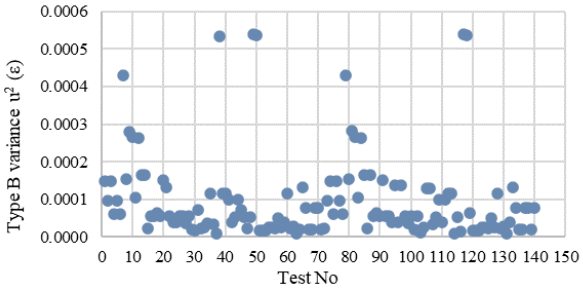

Figure 12. Type B uncertainty for strain at peak deviator stress

8. Combined standard uncertainty

Type A and type B uncertainty have now been calculated for each of the individual test results. Eq. (15) gives the combined uncertainty for peak deviator stress and Eq. (16) for strain at peak deviator stress, using the law of propagation of uncertainty.

$$u_C^2(\sigma_v) = u_A^2(\sigma_v) + u_B^2(\sigma_v) \quad (15)$$

$$u_C^2(\varepsilon) = u_A^2(\varepsilon) + u_B^2(\varepsilon) \quad (16)$$

As type A uncertainty, for both results, is higher than type B, it is evident that this will drive the final results.

8.1. Peak deviator stress combined uncertainty

The results of Eq. (15) are plotted in Fig. 13, which shows the combined uncertainty for peak deviator stress.

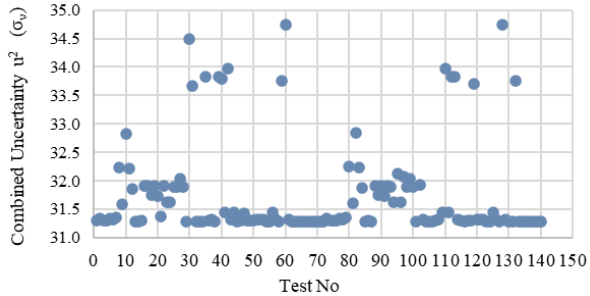

Figure 13. Combined uncertainty for peak deviator stress

Fig. 10 and 13 are identical in shape, with Fig. 13 shifted upwards by the amount of type A uncertainty.

8.2. Strain at peak deviator stress combined uncertainty

The results of Eq. (16) are plotted in Fig. 14, which shows the combined uncertainty for strain at peak deviator stress.

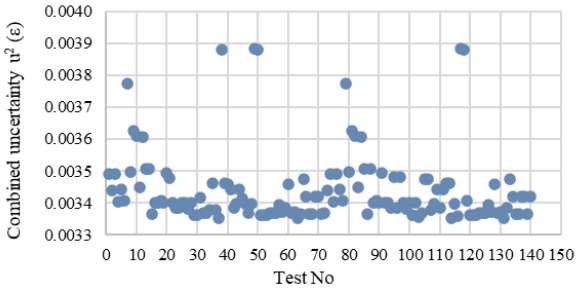

Figure 14. Combined uncertainty for strain at peak deviator stress

The impact of type A uncertainty is again the most significant. The slight variation is due to type B uncertainty, but all results have shifted to be almost equal to type A uncertainty.

9. Expanded uncertainty

9.1. Calculation of expanded uncertainty

According to Eq. (8), a coverage factor (k) must be chosen to calculate the expanded uncertainty. The coverage factor is generally based on the level of confidence required and the distribution followed by the measurement result.

9.2. Selection of coverage factor

Peak deviator stress and strain standard uncertainties are calculated from separate uncertainty factors, adding up to 16 for stress and 4 for strain. In both these cases, based on the central limit theorem, it can be safely assumed that the overall combined uncertainty follows the normal distribution (IPM et al. 2008).

Both deviator stress and strain results also follow a normal distribution, as described in Section 5.2.

Based on the above, normality can be assumed for the two measurands and their corresponding uncertainties. Therefore, a coverage factor of 2 will lead to a 95% level of confidence, and a coverage factor of 3 to a 99.7% level of confidence. A 95% level of confidence is normally acceptable in this this type of testing.

For each individual test result, the combined uncertainty is calculated as the positive square root of the combined variance. This is then multiplied by the coverage factor to yield the expanded uncertainty according to Eq. (17) and (18).

$$U(\sigma_v) = 2u_c(\sigma_v) \quad (17)$$

$$U(\varepsilon) = 2u_c(\varepsilon) \quad (18)$$

Expanded uncertainty is then averaged across all 140 tests. Percentage expanded uncertainty is also calculated for every test and averaged across all results.

9.3. Expanded uncertainty results

Fig. 15 and 16 show expanded uncertainty results, in terms of standard deviation, for peak deviator stress and strain at peak deviator stress respectively. Table 4 summarises all the uncertainty results, including uncertainty as a percentage.

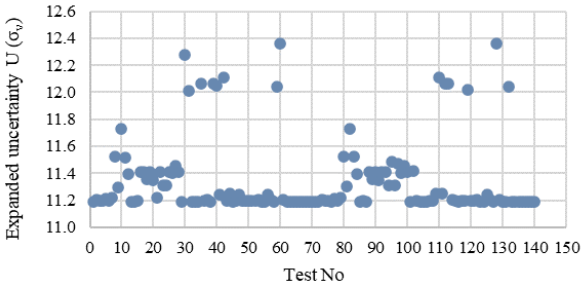

Figure 15. Expanded uncertainty for strain at peak deviator stress

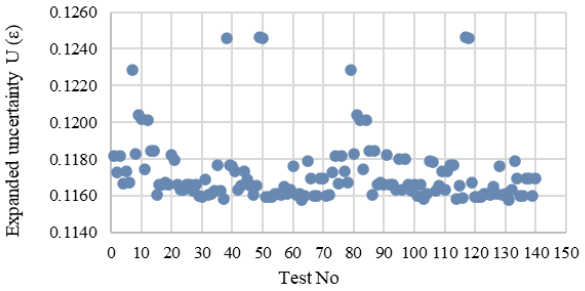

Figure 16. Expanded uncertainty for strain at peak deviator stress

Table 4. Final uncertainty results

	Peak deviator stress σ_v (kPa)	Strain ε (%)
Average test result	593	2.97
Average combined uncertainty u	5.7	0.059
Average expanded uncertainty U	11	0.117
Average percentage expanded uncertainty U	1.9 %	4.2 %

10. Discussion

10.1. Evaluation of results and conclusions

10.1.1. Equipment calibration uncertainty

The calibration results indicate a spread of uncertainty depending on the type of measuring equipment used. The equipment used in the laboratory varies in operating principle, make and model, capacity, and length of time in service. All these factors affect overall error and calibration uncertainty.

For load cells in particular, uncertainty and error increase towards the lower end of their capacity. This means that if a higher capacity load cell is used in a test, and the final load is less than 20% of its maximum capacity, the load uncertainty will be higher than that obtained using a lower capacity load cell, where the peak load was achieved above 20% of its maximum capacity.

Regarding volume, triaxial machines use two different types of devices: automatic volume change apparatus and pressure controllers. These operate differently and achieve different accuracies and uncertainties.

Calipers have three functions, measuring internal diameter, external diameter and depth, and these are calibrated separately. Each comes with different errors and different uncertainties, although these are not significant. Sample dimensions might be measured in any of these ways, and so the final error and uncertainty might vary slightly.

Deformation is usually measured externally and not directly on the sample. Minor variation from vertical direction as well as surface texture of the point where the transducer comes in contact with the frame, increase the measurement uncertainty.

Equipment uncertainty could be calculated more efficiently if the error had already been corrected. However, due to the nature of this type of test, Section 10.1.2 shows that this would not be expected to affect the overall results significantly.

10.1.2. Comparison between type A and type B uncertainty results

The difference between type A and B uncertainties in both peak deviator stress and strain at peak deviator stress was significant. All the uncertainties that contributed to the final test result through the measuring devices were essentially insignificant and had almost no effect on uncertainty. The most important factor appeared to be type A uncertainty, the random variability of repeated test results.

10.1.3. Overall uncertainty results

Table 2 shows 11 kPa (1.9%) uncertainty for peak deviator stress and 0.117 % (4.2%) uncertainty for strain at peak deviator stress. These results appear to be normal, and relatively low when the number of factors affecting the overall result is taken into account.

10.2. Considerations for further steps

This paper describes a methodology for calculating the peak deviator stress and strain uncertainty of isotropically consolidated triaxial compression tests on saturated non-cohesive soils. Some issues still remain to be addressed and considered.

The specimen's dry density was prescribed between 1.58 and 1.62 gr/cm^3. No record was kept of the exact achieved density of each specimen, adding an extra uncertainty parameter. To increase the reliability of the uncertainty results, this should be quantified either by ensuring that all test results are performed with the exact same dry density or by dividing the comparisons for each density value. The same applies to the initial water content, which also strongly influences initial bulk and dry density. However, as the sample is saturated, its overall effect is probably insignificant.

The Ladd (1978) undercompaction method attempts to produce homogenous specimens, but this is only an indication and is not verified. If (some) specimens do not have a uniform structure throughout, this could be a parameter potentially affecting uncertainty.

The layout of the experiment indicates uncertainty in a very narrow range of triaxial test results and conditions. As only one material was tested, no assumptions can be made about the behaviour of coarser or finer sands, or how the same material will behave in different densities and under different pressures, or what the uncertainty for undisturbed cohesive samples will be. Each of these is a separate exercise on its own.

Significantly, initial sample height was assumed to be the height calculated at the end of consolidation rather than the actual initial height measured at the beginning of the test. As the focus was on the shear stress of the sample, the effect of this is expected to be minor and to be reduced further based on the conclusions regarding type A and B uncertainties above. Nevertheless, the initial height uncertainty should be added to the change in height uncertainty during the consolidation stage to obtain the overall height uncertainty at the beginning of the shearing stage

All the tests specify a cell pressure to be achieved. The actual cell pressure achieved, and whether it was different from the target, has not been verified. As the results passed the laboratory's quality assurance checks, even if they deviated, any difference would only have been a few kPa. But even a small variation in cell pressure is expected to influence the test results and their respective uncertainties.

Finally, the shear stress of the membrane used to confine the sample was not considered. The ISO 17892-9:2018 (ISO 2018) standard specifies a nominal shear stress to be used, and the peak deviator stress is then adjusted based on the membrane thickness and the strains that occur in the sample. The results are in the region of a few kPa and thus, assuming the uncertainty is of the same order of magnitude as for the sample, probably have insignificant influence on the sample's peak deviator stress uncertainty. But it would be worth carrying out tests to measure both the membrane's deviator stress and the corresponding uncertainty.

Acknowledgements

The author is grateful to Manolis Mathioulakis, Helen Gough, Damien Christiaens, Tim Carrington and Ian Nicholson for their valuable feedback and advice and to Fugro's laboratory personnel in Wallingford, UK for performing and processing the tests.

References

International Organization for Standardization [ISO]. 2018) "Geotechnical investigation and testing – Laboratory testing of soil – Part 9: Consolidated triaxial compression tests on water saturated soils (ISO 17892-9:2018)". https://www.iso.org/standard/70954.htm

International Organization for Standardization [ISO]. 2023. "Accuracy (trueness and precision) of measurement methods and results - Part 1: General principles and definitions (ISO 5725-1:2023)". https://www.iso.org/standard/69418.html

IPM, IEC, IFCC, ILAC, ISO, IUPAC, IUPAP, and OIML. 2008. "Evaluation of measurement data – Guide to the expression of uncertainty in measurement". Joint Committee for Guides in Metrology, JCGM 100:2008. https://www.bipm.org/documents/20126/2071204/JCGM_100_2008_E.pdf/cb0ef43f-baa5-11cf-3f85-4dcd86f77bd6.

Ladd, R. 1978. "Preparing test specimens using undercompaction." Geotech. Test. J., 1(1), pp. 16-23.

Mathioulakis, M. 2004. *Μέτρηση, ποιότητα μέτρησης και αβεβαιότητα* [Measurement, measurement quality, and uncertainty]. Ilisia: HellasLab. ISBN 960-88226-0-2.